

# Excess spontaneous-emission factor in unstable-resonator lasers

Gang Yao and Y. C. Chen

*Department of Physics and Astronomy, Hunter College of The City University of New York, 695 Park Avenue, New York, New York 10021*

C. M. Harding, S. M. Sherrick, R. J. Dalby, and R. G. Waters

*McDonnell Douglas Electronic Systems Company, Elmsford, New York 10523*

C. Largent

*Phillips Laboratory, Kirtland Air Force Base, New Mexico 87117-6008*

Received April 10, 1992

The spontaneous-emission factor in an unstable-resonator semiconductor laser is enhanced by more than 2 orders of magnitude compared with that of a Fabry-Perot semiconductor laser having the same volume. A clear linkage has been observed among the spontaneous-emission factor, the waveguiding property, and the width of the lasing spectral envelope.

The unstable-resonator laser has been studied extensively since the early years of laser development.<sup>1</sup> Its high-power performance owing to the large gain volume and its good beam quality in the far field owing to better discrimination against higher-order transverse modes make the unstable resonator a useful cavity structure for high-power solid-state lasers. In semiconductor lasers, the magnifying effect of the unstable-resonator cavity has been reported to be effective in counterbalancing the self-focusing effect of lasing filaments and producing nearly diffraction-limited beams.<sup>2,3</sup> Issues related to the laser cavity design and modal characteristics also have been analyzed.<sup>2,3</sup>

The unstable resonator belongs to the class of laser cavities that may possess an excess spontaneous-emission factor<sup>4</sup> owing to the nonorthogonal transverse modes.<sup>5-7</sup> The spontaneous-emission factor, defined as the fraction of the spontaneous emission coupled into the lasing mode, plays an important role in determining the spectral purity and temporal coherence of the laser emission.<sup>8</sup> In semiconductor lasers, it also contributes to a damping factor of the relaxation oscillation and affects the dynamic behavior of lasers.<sup>9</sup> Generally speaking, the spontaneous-emission factor is inversely proportional to the volume of the gain medium.<sup>4</sup> This factor is higher in semiconductor lasers owing to the smaller size of the laser. In lasers with gain-induced waveguiding or with an open cavity, additional enhancement of the spontaneous-emission factor may occur.<sup>4,5,10,11</sup> This excess spontaneous-emission factor in the gain-guided semiconductor lasers is responsible for the multiple-longitudinal-mode operation in the homogeneously broadened system.<sup>8</sup> Whereas the existence of an excess spontaneous-emission factor in the unstable-resonator lasers has been discussed in recent publi-

cations,<sup>6,7</sup> thus far there has been no experimental study on this subject.

In this Letter we present results of an experimental study of the spontaneous-emission factor in unstable-resonator semiconductor lasers. The spontaneous-emission factor in an unstable-resonator laser having a convex mirror with 2.2-mm radius of curvature is measured to be  $2 \times 10^{-3}$  as compared with an expected value of  $10^{-5}$  in a Fabry-Perot semiconductor laser with the same dimensions. The large enhancement of the spontaneous-emission factor is in agreement with the values estimated from the laser cavity parameters. Lasers with an excess spontaneous-emission factor also operate in multilongitudinal modes above the threshold. A linkage among the spontaneous-emission factor, the cavity structure, and the longitudinal-mode spectra has been observed. In addition, we have observed a drastic reduction in the spontaneous-emission factor by as much as 2 orders of magnitude owing to the development of thermal waveguiding.

The unstable-resonator semiconductor lasers used in this study consist of a laser structure with monolithically stacked graded-index separate-confinement heterostructure single-quantum-well laser with three optically coupled waveguides.<sup>12</sup> One cavity mirror is formed by natural cleavage, and the other is a convex mirror fabricated by chemically assisted ion-beam etching. The radius of curvature is 2.2 mm, corresponding to a round-trip magnification of 6.9. With the use of a stripe width of 100  $\mu\text{m}$ , the gain-induced waveguiding can be neglected, and the curvature of the wave front of the laser beam near the center of the stripe is determined solely by the curvature of the laser mirror. The laser structure is illustrated schematically in Fig. 1. By applying the geometrical-optics analysis to the unstable resonator, the virtual source as

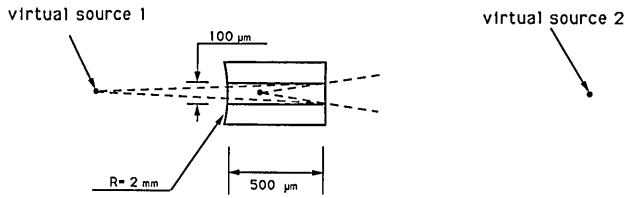


Fig. 1. Geometry of the unstable-resonator semiconductor laser used in this study.

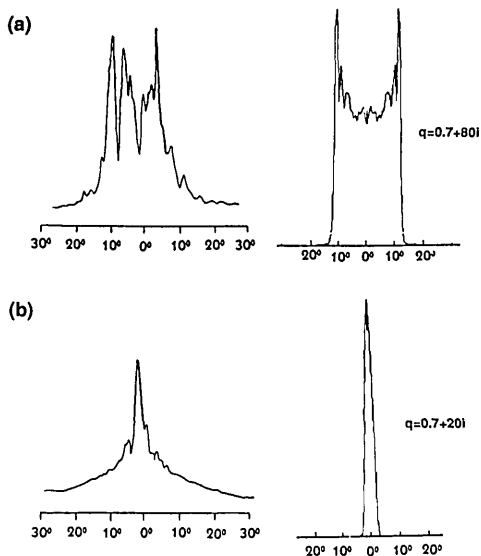


Fig. 2. Measured (left) and calculated (right) far-field intensity distribution of an unstable-resonator semiconductor laser, measured at 1.1 cm in front of the facet with no imaging optics, when the laser is operated in (a) pulsed and (b) cw conditions. Note that the laser is operated at  $1.05I_{th}$ . The broad background is caused by the spontaneous emission.

viewed from the side of the planar mirror is 0.31 mm behind the facet. This is in close agreement with the observed astigmatism of 0.3 mm when the laser is operated in the pulsed condition. The geometrical parameters of the laser are illustrated in Fig. 1.

Under pulsed operation with 400-ns-long pulses, the unstable-resonator laser operates in a large number of longitudinal modes. The adjacent longitudinal modes are separated by 0.35 nm. The lateral far-field patterns, measured at a 1.1-cm distance in front of the virtual source with no imaging optics, typically exhibit two major lobes with many peaks in between whose intensity envelopes have a depression at the center as shown in Fig. 2(a). A detailed examination of the longitudinal-mode spectrum shows no signature of fine structures, indicating single-lateral-mode operation. In contrast, the longitudinal-mode spectrum of a typical Fabry-Perot laser with the same stripe width exhibits fine structures owing to the multilateral mode operation. The multiple peaks in the far-field pattern are believed to be caused by the aberration when the wave front in the wings deviates considerably from the cylindrical (Gaussian) shape owing to propagation in the lossy region outside the stripe. In this case, the wave front can be better approximated by a sech function<sup>13,14</sup> rather than a Gaussian function. The

cw far-field pattern, as shown in Fig. 2(b), is single lobed with much smaller beam divergence. We attribute the changes in the beam characteristics to the thermal waveguiding effect under the cw operation.<sup>14,15</sup> The pulsed-to-cw transition time constant is much longer than 20  $\mu$ s, the upper limit of our pulse generator.

To determine the spontaneous-emission factor, the power of one of the longitudinal modes near the peak of the gain spectrum is measured as a function of the injection current. A grating spectrometer is used to select the modes. The slit width of the spectrometer is adjusted so that the total emission within a 0.2-nm window is collected. The spontaneous-emission factor is determined by comparing the experimental data with the theoretical curves calculated based on the multimode rate equations for photon and carrier densities. Figure 3 shows the measured spontaneous-emission power of the central mode as a function of normalized injection current for an unstable-resonator laser in the pulsed and cw conditions. As a reference, the data taken in a Fabry-Perot ridge-waveguide laser with a 5- $\mu$ m stripe width and a 600- $\mu$ m cavity length are also plotted. By comparison with the theoretical curves, the spontaneous-emission factor is  $2 \times 10^{-3}$  for the unstable-resonator laser in the pulsed condition and  $1 \times 10^{-5}$  in the cw condition. The value for the 5- $\mu$ m-wide ridge-guide laser is  $8 \times 10^{-5}$ . To the extent that the spontaneous-emission factor is inversely proportional to the modal volume, the value for a Fabry-Perot laser with 100- $\mu$ m width and 500- $\mu$ m length would be  $4 \times 10^{-6}$ . The open cavity of the unstable resonator results in an enhancement factor of 500.

The enhanced spontaneous-emission factor in the unstable resonator cavity is due to the nonorthogonality of the transverse modes in lasers with either gain guiding<sup>4,5,10,11</sup> or, in the present case, an open cavity. The spontaneous emission  $\beta$  can be expressed as<sup>6,7</sup>

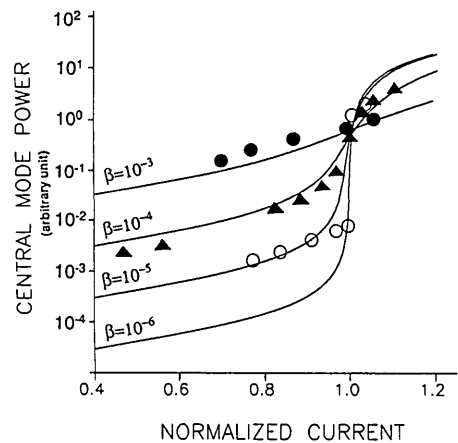


Fig. 3. Output power of the central mode near the peak of the gain as a function of normalized injection current for an unstable-resonator laser operated in the pulsed (filled circles) and cw (open circles) conditions and for a 5- $\mu$ m-wide ridge-guide Fabry-Perot laser (triangles). The solid curves are the results calculated based on the rate equations.

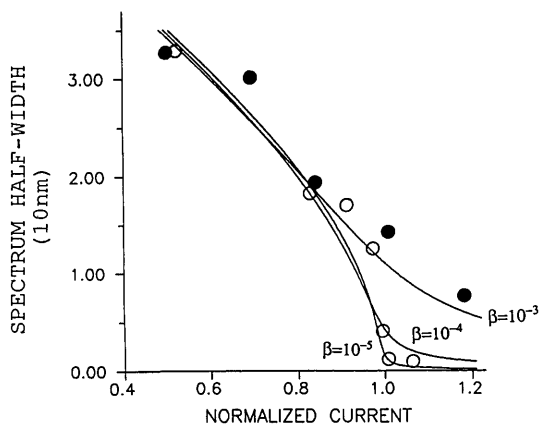


Fig. 4. Half-width of the laser spectral envelope as a function of injection current for an unstable-resonator laser in the pulsed (filled circles) and cw (open circles) modes of operation.

$$\beta = \beta_0 K_L K_T, \quad \beta_0 = \lambda^4 / 4\pi^2 V_{\text{eff}} \Delta\lambda_{\text{sp}} n^3, \quad (1)$$

where  $\beta_0$  is the spontaneous-emission factor for an ideal closed-cavity laser without cavity loss and transverse-mode nonorthogonality,  $K_L$  is the enhancement factor caused by the nonorthogonality of the longitudinal modes in the presence of cavity losses, and  $K_T$  is the enhancement factor that is due to the nonorthogonality of the transverse mode,  $V_{\text{eff}}$  is the effective modal volume,  $\Delta\lambda_{\text{sp}}$  is the spectral width of the spontaneous emission, and  $n$  is the refractive index. Using  $\lambda = 830$  nm,  $V_{\text{eff}} = 100 \mu\text{m} \times 500 \mu\text{m} \times 0.4 \mu\text{m}$ ,  $\Delta\lambda_{\text{sp}} = 30$  nm, and  $n = 3.6$ , we calculate  $\beta_0$  to be  $0.7 \times 10^{-6}$ . The  $K$  factors are

$$K_L = \frac{1}{|\gamma|^2} \left[ \frac{1 - |\gamma|^2}{\ln(1/|\gamma|^2)} \right]^2, \quad \gamma = \frac{r_1 r_2}{\sqrt{M}}, \quad (2)$$

$$K_T = \frac{\left[ \int \phi^*(x) \phi(x) dx \right]^2}{\left| \int \phi^2(x) dx \right|^2}, \quad (3)$$

where  $\gamma$  is the cavity loss,  $M$  is the magnification factor,  $r_1$  and  $r_2$  are reflectivity of the mirrors,  $\phi$  is the field distribution of the lasing mode at the plane of symmetry, and the integration is carried out in the lateral direction.

To estimate the  $K_T$  factor, we approximate the spatial profile  $\phi$  in the lateral direction at the facet by a sech function of the form<sup>13,14</sup>

$$\phi = \phi_0 \text{sech}^q(x/w), \quad q = q_R + iq_I, \quad (4)$$

where  $w$  is the stripe width and the parameters  $q_R = 1$  and  $q_I = \pi n w^2 / \lambda R$  are determined by requiring that the Taylor series expansion of the near field near  $x = 0$  gives rise to a cylindrical wave front with a radius of curvature of  $R$ . Using  $r_1^2 = r_2^2 = 0.3$  and  $M = 6.9$  for the unstable resonator, we obtain  $q = 0.7 + 80i$ ,  $K_T = 175$ ,  $K_L = 4$ , and  $\beta = 5 \times 10^{-4}$  for the pulsed operation. For a Fabry-Perot resonator with the same dimensions,  $M = 1$ ,  $K_T = 1$ ,  $K_L = 1.8$ , and  $\beta = 1 \times 10^{-6}$ . The enhancement factor caused by the open cavity is 500. For the cw operation, the far-field pattern can be ap-

proximated by  $q = 0.7 + 20i$ , which leads to  $K_T = 15$  and  $\beta = 1 \times 10^{-5}$  or a 50-fold reduction in the spontaneous-emission factor.

The excess spontaneous emission also results in a broader lasing spectral envelope with as many as 30 longitudinal modes within the FWHM envelope. This effect is illustrated in Fig. 4. The onset of thermal waveguiding reduces the spontaneous emission factor and results in nearly single-mode emission in the cw condition. The general feature of the lasing spectrum width as a function of the injection current can be explained by a modeling, represented by the solid curves in Fig. 4, based on the multimode rate equations. These phenomena are reminiscent of those observed in gain-guided semiconductor lasers.<sup>8</sup>

In conclusion, we have characterized the spontaneous-emission factor in an unstable-resonator semiconductor laser. The open-cavity configuration results in an enhancement of 2 orders of magnitude in the spontaneous-emission factor. The development of thermal waveguiding under cw operation results in a significant reduction in the spontaneous-emission factor. We have observed a clear linkage between the spontaneous-emission factor and the width of the lasing spectral envelope. With the large spontaneous-emission factor, the unstable-resonator laser is expected to be dynamically stable against relaxation oscillations and other intensity instabilities. However, the development of thermal waveguiding can significantly affect the stability of the laser beam.

## References

1. A. E. Siegman, *Lasers* (University Science, Mill Valley, Calif., 1986), Chaps. 21–23 and p. 815.
2. J. Salzman, T. Venkatesan, R. Lang, M. Mittelstein, and A. Yariv, *Appl. Phys. Lett.* **46**, 218 (1985); R. J. Lang, M. Mittelstein, A. Yariv, and J. Salzman, *IEEE Proc.* **135**, 69, 76 (1987).
3. M. L. Tilton, G. Dente, A. H. Paxton, J. Cser, R. K. Defreez, C. E. Moeller, and D. Depatie, *IEEE J. Quantum Electron.* **27**, 2098 (1991).
4. K. Petermann, *IEEE J. Quantum Electron.* **QE-15**, 566 (1979).
5. A. Yariv and S. Margalit, *IEEE J. Quantum Electron.* **QE-8**, 1831 (1982).
6. A. E. Siegman, *Phys. Rev. A* **39**, 1253, 1264 (1989).
7. P. L. Mussche and A. E. Siegman, *Proc. Soc. Photo-Opt. Instrum. Eng.* **1376**, 153 (1990).
8. W. Streifer, D. R. Scifres, and R. D. Burnham, *Appl. Phys. Lett.* **40**, 305 (1982).
9. Y. Suematsu, S. Akiba, and T. Hong, *IEEE J. Quantum Electron.* **QE-13**, 596 (1977).
10. M. Newstein, *IEEE J. Quantum Electron.* **QE-20**, 1270 (1984).
11. C. H. Henry, *IEEE J. Lightwave Technol.* **LT-4**, 288 (1986).
12. R. G. Waters, Y. C. Chen, and R. J. Dalby, *Proc. Soc. Photo-Opt. Instrum. Eng.* **1219**, 69 (1990).
13. P. M. Asbeck, D. A. Cammack, and J. J. Daniele, *Appl. Phys. Lett.* **33**, 504 (1978).
14. Y. C. Chen, A. R. Reisinger, and D. Pense, *IEEE J. Quantum Electron.* **QE-19**, 1092 (1983).
15. Y. C. Chen, A. R. Reisinger, and S. R. Chinn, *Appl. Phys. Lett.* **41**, 129 (1983).